Form and function in a sample of platyrrhine primates:
A three-dimensional analysis of dental and TMJ morphology

Siobhán B. Cooke[1] and Claire E. Terhune[2]

[1]Department of Anthropology, Northeastern Illinois University

[2]Department of Community and Family Medicine, Duke University School of Medicine

Introduction

As integral parts of the masticatory apparatus, the morphology of the dentition and skull, and particularly the temporomandibular joint (TMJ), should be tightly linked. Fine control over condylar and mandibular movements guides the teeth into occlusion, while the topography and position of the dental arcade mediate mandibular movements. The dentition, as the portion of the masticatory apparatus that is most directly involved in triturating food items, has been shown to strongly reflect dietary regimes (e.g., Kay 1975; Rosenberger and Kinzey 1976; Anapol and Lee 1999; Boyer 2008; Cooke 2011). Similarly, cranial form is correlated with differences in feeding behavior among taxa (e.g., Shea, 1983; Antón 1996; Taylor 2002, 2005; Norconk et al. 2009) and TMJ shape has been shown to reflect joint reaction forces and joint range of motion, both of which vary in relation to feeding strategy (Bouvier 1986a,b; Wall 1999; Vinyard et al. 2003; Terhune 2011a,b). Although numerous studies have documented links between tooth form and diet, and cranial/TMJ shape and feeding behavior, to date no study has systematically examined covariance between these two systems. **The goal of this study was to employ three-dimensional geometric morphometric techniques to examine detailed morphological data from both of these regions.** We examine this covariation in a sample of platyrrhine primates, a clade which displays a range of dietary regimes and body sizes, and in which masticatory and dental variation is well documented (e.g., Rosenberger 1992; Ford and Davis 1992). **We predict that masticatory, and particularly TMJ, morphology and dental shape covary significantly in platyrrhine primates.**
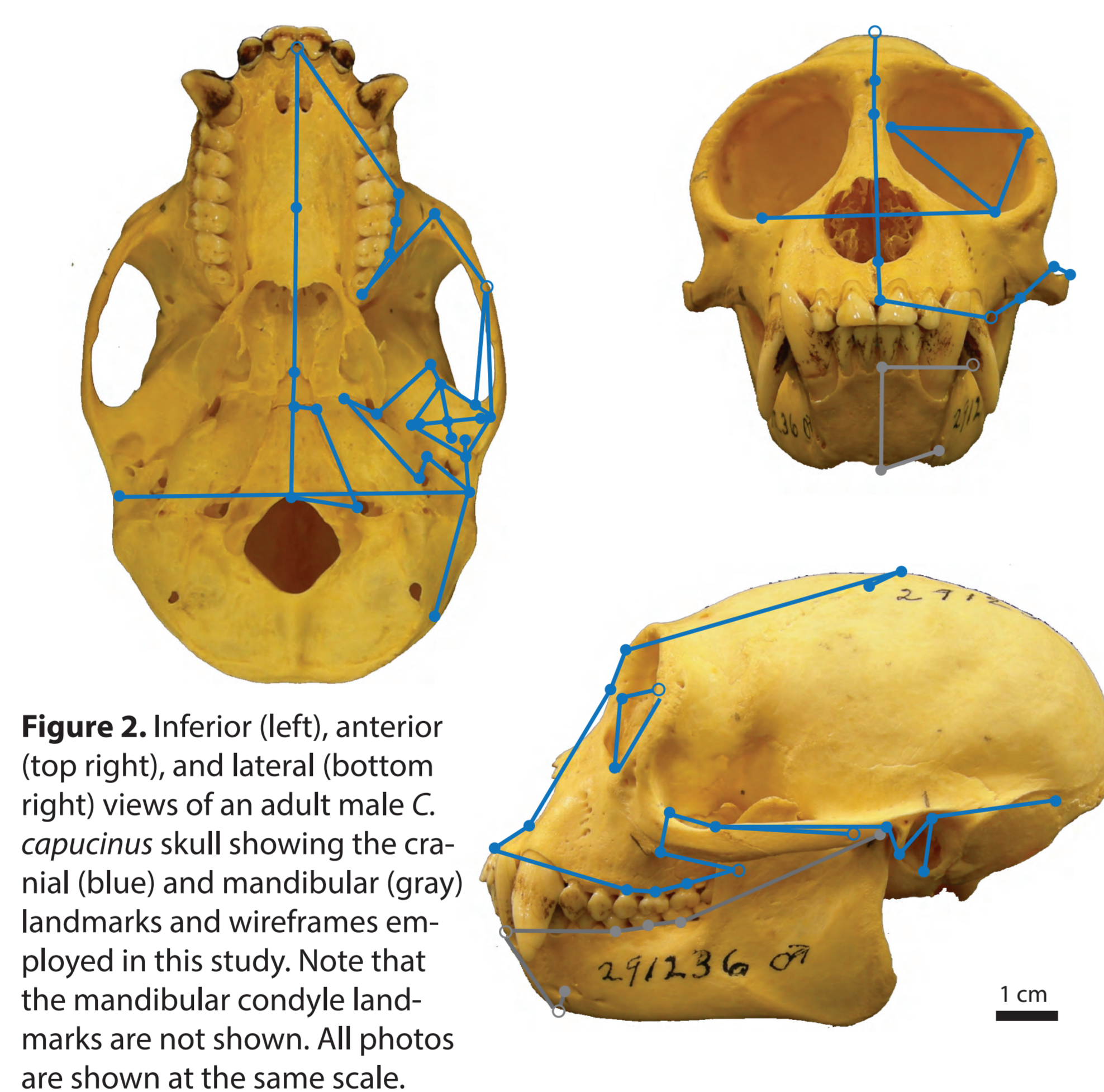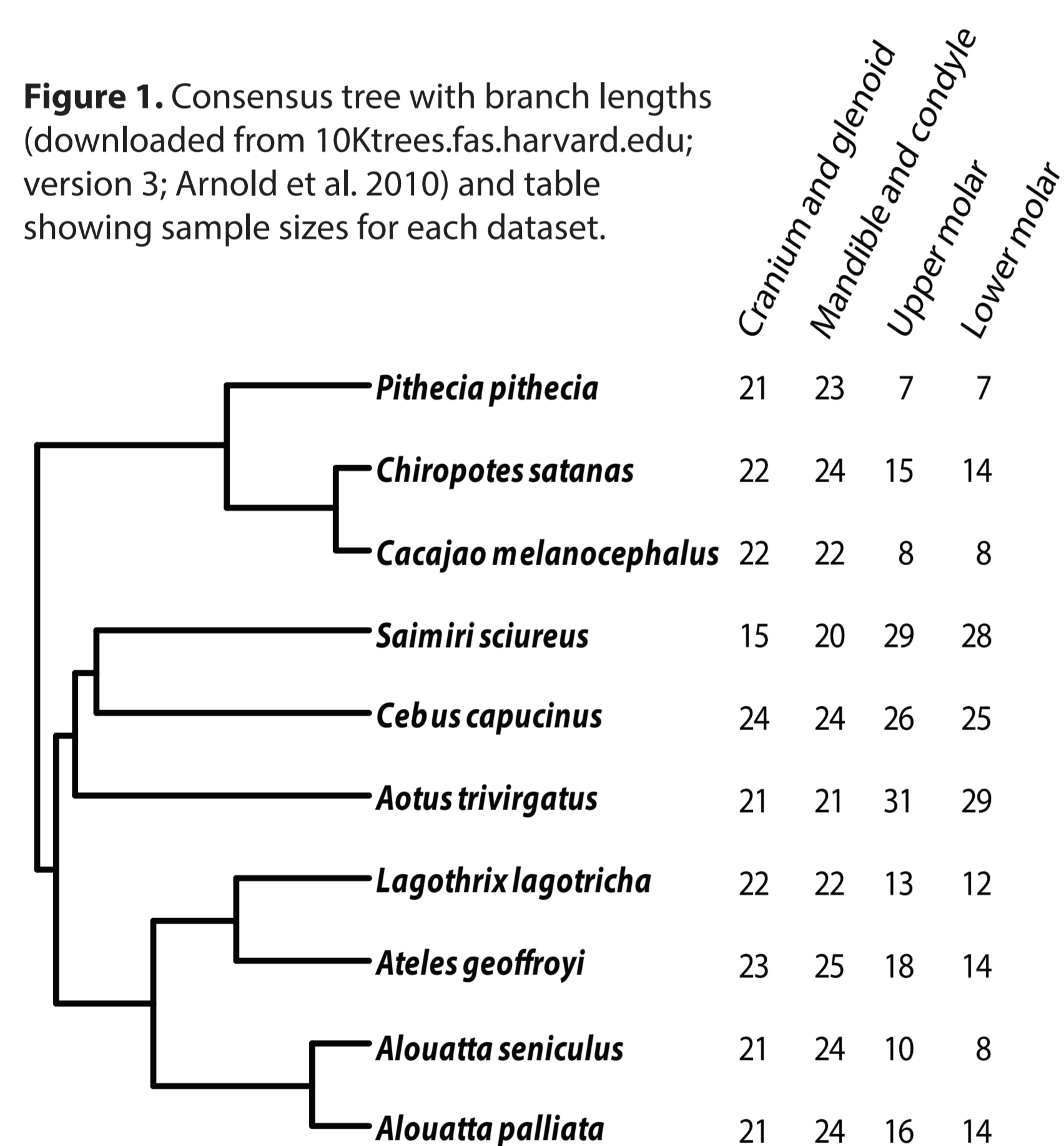
Materials and Methods

Three-dimensional x,y,z coordinate landmarks were collected on the crania and dentition of a mixed sex sample of ten platyrrhine species (Fig. 1-3). Six datasets were created from these landmark sets: upper molar, lower molar, cranium and glenoid, glenoid only, mandible and condyle, and condyle only.

For each of the six datasets, we performed the following analyses in the program R (R Development Core Team 2008) using the package 'geomorph' (Adams and Otárola-Castillo 2012):

- Mean forms were calculated for each species and superimposed using Generalized Procrustes Analysis.
- The phylogenetic signal was calculated and its significance assessed using a permutation test (9,999 iterations). We visualized this signal by overlaying the consensus tree on a plot of principal component (PC) axes 1 and 2.
- Allometry in the dataset was assessed by regressing the Procrustes aligned coordinates ('shape') on the natural log of mandible length with (PGLS) and without a consideration of phylogenetic covariance.

To examine covariation among the six datasets we performed two-block partial least squares (2B-PLS) analyses using the size and phylogeny adjusted regression residuals; shape variation along each PLS axis was examined using wireframe diagrams.

Figure 1. Consensus tree with branch lengths (downloaded from 10Ktrees.fas.harvard.edu; version 3; Arnold et al. 2010) and table showing sample sizes for each dataset.

	Cranium and glenoid	Mandible and condyle	Upper molar	Lower molar
Pithecia pithecia	21	23	7	7
Chiropotes satanas	22	24	15	14
Cacajao melanocephalus	22	22	8	8
Saimiri sciureus	15	20	29	28
Cebus capucinus	24	24	26	25
Aotus trivirgatus	21	21	31	29
Lagothrix lagotricha	22	22	13	12
Ateles geoffroyi	23	25	18	14
Alouatta seniculus	21	24	10	8
Alouatta palliata	21	24	16	14

Figure 2. Inferior (left), anterior (top right), and lateral (bottom right) views of an adult male *C. capucinus* skull showing the cranial (blue) and mandibular (gray) landmarks and wireframes employed in this study. Note that the mandibular condyle landmarks are not shown. All photos are shown at the same scale.
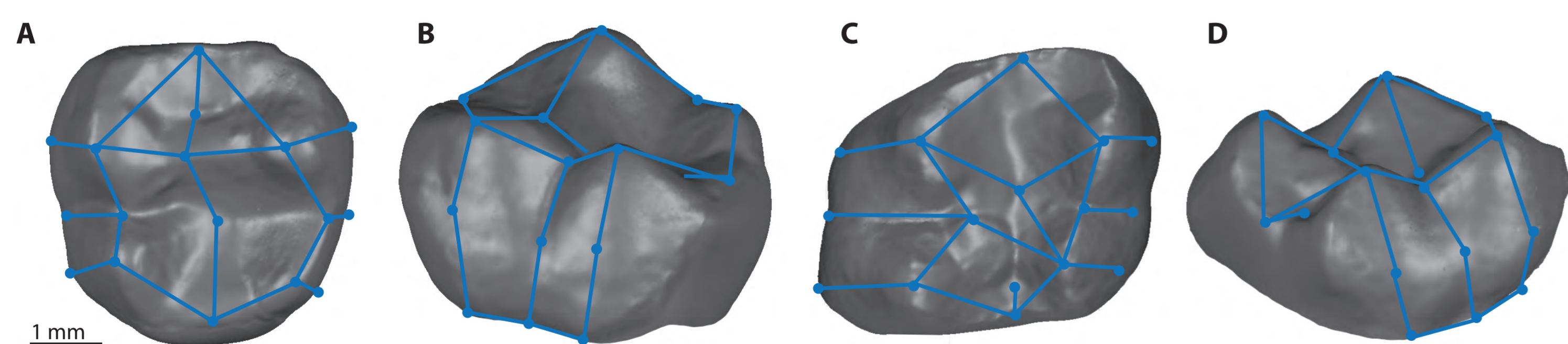
Figure 3. Laser-scan generated images of the mandibular and maxilary molars of *C. capucinus* showing landmarks and wireframes used in this study. A) occlusal view of mandibular molar, mesial to the top, buccal to the left; B) oblique view of mandibular molar from a distobuccal perspective; C) occlusal view of maxillary molar, mesial to the top, lingual to the left; D) oblique view of maxillary molar from a distobuccal perspective.

References

Adams DC, Otárola-Castillo E. 2012. 'geomorph' R package version 1.0. Anapol F, Lee S. 1994. AJPA 94, 239–261. Antón, S. 1996. Int J Prim 17, 401-427. Arnold CLJ, Matthews L, Nunn CL. 2010. Evol Anth 19, 114-118. Bouvier M. 1986a. AJPA 69, 473-482. Bouvier M. 1986b. Int J Prim 7, 551-567. Boyer DM. 2008. JHE 55, 1118–1137. Cooke SB. 2011. Anat Rec 294, 2073-2091. Ford SM, Davis LC. 1992. AJPA 88, 415–468. Kay RF. 1975. AJPA 43, 195–216. Norconk M, et al. 2009. In: Garber et al. (eds.), South American Primates: Testing New Theories in the Study of Primate Behavior, Ecology, and Conservation. Springer Science, New York, pp. 279-319. Rice WR. 1989. Evolution 43, 223-225. Rosenberger AL, Kinzey WG. 1976. AJPA 45, 281–298. Rosenberger AL. 1992. AJPA 88, 525–562. Ross CF, Ravosa M. 2003. AJPA 91,305-324. Shea BT. 1983. Fol Primatol 40, 32-68. Taylor AB. 2002. AJPA 117,113-56. Taylor AB. 2005. JHE 48,555-574. Terhune CE. 2011a. JHE 61, 583-596. Terhune CE. 2011b. J Anat 219, 551-564. Vinyard C, et al. 2003. AJPA 120,153-170. Wall C. 1999. AJPA 109, 67-88.
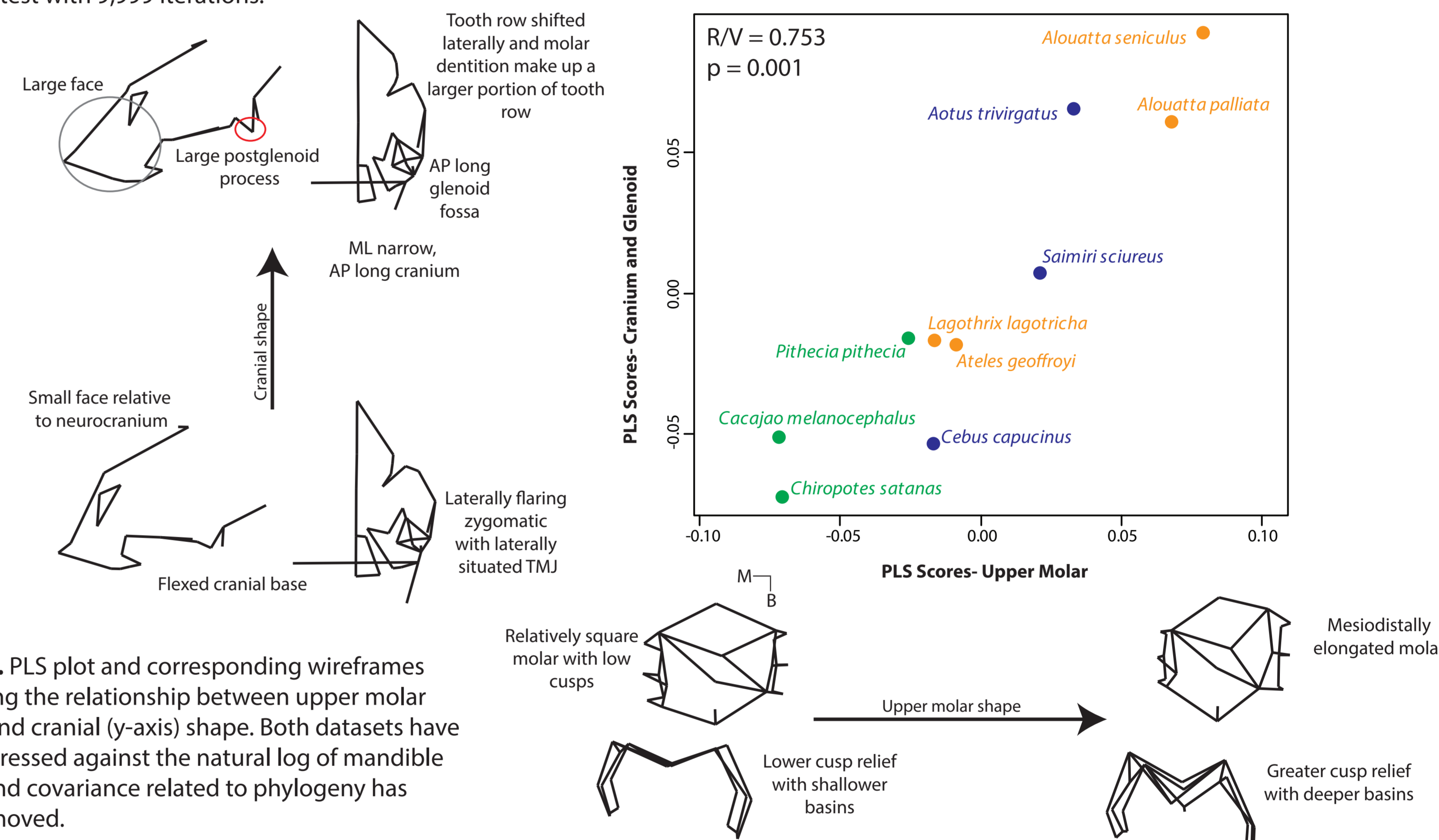
Results

	Phylo. signal	p-value
Upper molars	0.041	**0.001**
Lower molars	0.052	**0.004**
Cranium and glenoid	0.067	**0.002**
Glenoid	0.035	**0.003**
Mandible and condyle	0.009	**0.004**
Condyle	0.038	0.386

Table 1. A significant phylogenetic signal (bolded p-values) was found for all datasets except the mandibular condyle.

	Shape ~ Ln (Mand. Length) (No phylo. correction)		Shape ~ Ln (Mand. Length) (Brownian motion PGLS)	
	%variance	p-value	%variance	p-value
Upper molars	18.79	0.085	18.31	0.387
Lower molars	14.50	0.242	13.89	0.530
Cranium and glenoid	38.73	**0.005**	32.77	0.121
Glenoid	28.46	**0.006**	22.26	0.280
Mandible and condyle	22.51	0.107	11.14	0.624
Condyle	16.27	0.209	9.90	0.689

Table 2. Results of the regression analyses of shape against the natural log of mandible length with and without phylogenetic correction. Only cranial and glenoid shape are significantly correlated with mandible length, and only when phylogeny is not incorporated into the analysis. Significance of the regressions was assessed using a permutation test with 9,999 iterations.

Figure 4. PC plots for the upper molar (top) and cranium/glenoid fossa (bottom); both plots include an overlay of a consensus phylogenetic tree to illustrate the relationship between shape and phylogeny.

Figure 5. PLS plot and corresponding wireframes illustrating the relationship between upper molar (x-axis) and cranial (y-axis) shape. Both datasets have been regressed against the natural log of mandible length and covariance related to phylogeny has been removed.

		Cranium and glenoid	Glenoid only	Mandible and condyle	Condyle only
Lower molars	R/V	**0.712**	**0.789**	**0.860**	0.358
	p-value	**0.002**	**0.001**	**0.0002**	0.178
Upper molars	R/V	**0.753**	**0.784**	**0.706**	0.376
	p-value	**0.001**	**0.001**	**0.001**	0.317

Table 3. Results of the 2B-PLS analyses using the PGLS regression residuals of shape regressed on Ln mandible length. Bolded values are significant after sequential Bonferroni correction (Rice 1989). All analyses are significant except for the relationships between dental and condylar shape. The significance of this relationship was assessed using a permutation test with 9,999 iterations.

Discussion and Conclusions

This study examined cranial and dental covariation in platyrrhine primates. By using PGLS regression we were able to control for phylogenetic covariance, and by regressing shape on mandible length we standardized all of the datasets using a biomechanically significant scaling variable.

For example, the 2B-PLS plot illustrating the relationship between cranial and upper molar shape indicates that cusp relief and mesiodistal tooth length covary with cranial base flexion, face size, flaring of the zygomatics, and position of the TMJ relative to the tooth row.

- Although cranial shape differs substantially among these taxa, by controlling for size variation and phylogeny, smaller-bodied taxa that are more insectivorous (e.g., *Saimiri*) are revealed to be relatively similar in dental and cranial form to larger bodied folivorous taxa such as *Alouatta*. Interestingly, the small bodied nocturnal *Aotus* also appears similar to *Alouatta* in dental and cranial form. This similarity may be a result of a convergence in cranial form and basicranial flexion (Ross and Ravosa 1993) linked to the visual adaptations of *Aotus*; further analysis is warranted.
- Conversely, *Chiropotes* and *Cacajao*, two taxa that are well known for sclerocarp foraging and consumption of hard foods (Norconk et al. 2009), cluster on the negative ends of both PLS axes, and exhibit highly flexed crania, laterally flaring zygomatic arches, laterally positioned TMJs relative to the tooth row, and low-cusped dentition. This TMJ position and cusp morphology acts to increase bite forces and disperse forces over a larger area.
- What is perhaps most intriguing about this analysis is that the observed patterns of covariance between cranial and dental form do not fall along a gradient of dietary resistance, as has been demonstrated in platyrrhine primates previously (e.g., Norconk et al. 2009). Instead, this analysis separates taxa that utilize tough foods (e.g., *Alouatta*) and hard foods (e.g., *Chiropotes*), and more generalized (i.e., frugivorous) taxa are intermediate in form. This result suggests that perhaps coupling datasets may better elucidate the complex ways in which cranial and dental form interact during feeding.

While the finding that cranial/TMJ and dental shape covary in platyrrhines is not a surprising result, it is one that has not been previously demonstrated. With this information in hand, we can begin to explore the ways in which morphological covariation correlates with diet, phylogeny, body size or other variables pertinent to an organism's ecological adaptations. Additionally, while it is tempting to attribute these findings to functional differences among taxa, other explanations (e.g., modularity) must be also kept in mind.